

RESEARCH ARTICLE

The allometry of mitochondrial efficiency is tissue dependent: a comparison between skeletal and cardiac muscles of birds

Jessica Barbe[‡], Julia Watson, Damien Roussel* and Yann Voituron*

ABSTRACT

Body mass is known to be a fundamental driver of many biological traits, including metabolism. However, the effect of body mass on mitochondrial energy transduction is still poorly understood and has mainly been described in mammals. Using 13 species of birds ranging from 15 g (finches) to 160 kg (ostrich), we report here that the mitochondrial production of ATP, and the corresponding oxygen consumption, are negatively dependent on body mass in skeletal muscles but not in the heart. Results also showed that mitochondrial efficiency was positively correlated with body mass at sub-maximal phosphorylating states in the skeletal muscle, but not in the heart. This difference between muscle tissues is potentially linked to the difference in energetic demand expandability and the heavy involvement of skeletal muscle in thermoregulation.

KEY WORDS: Bioenergetics, Endotherms, ATP/O, Body mass, Metabolic scope, Phylogeny

INTRODUCTION

Body mass (M_h) is certainly one of the most fundamental and significant elements that characterize an organism's morphological, behavioral, physiological and ecological properties (Calder, 1996; Demetrius, 2006; Peters, 1983). Allometry, or the biology of scaling to body mass, is particularly useful in comparative biology and has been extensively explored across the full domain of life (Hatton et al., 2019; Hulbert et al., 2007; Peters, 1983; West and Brown, 2004, 2005; White et al., 2019). Metabolism sustains life by processing energy intakes from the environment into usable cellular energy that an organism can ultimately allocate to various functions depending on biological/ecological constraints (Glazier, 2015a; Koch et al., 2021). The equation describing the influence of body mass on basal and standard metabolism is Metabolic rate= aM_b^b , where a is the normalizing coefficient and b is the scaling exponent depending on metabolic activity and phylogenetic status (Demetrius, 2006; Glazier, 2015a, 2022). Studies focused on the subcellular level have reported that interspecific variation in body mass affects numerical aspects of mitochondrial bioenergetics, such as oxidative and phosphorylation capacities, membrane proton conductance, and reactive oxygen species (ROS) production (Boel et al., 2019; Brand et al., 2003; Darveau et al., 2002; Else et al., 2004; Emmett and Hochachka, 1981; Hulbert

Université Claude Bernard Lyon 1, CNRS, ENTPE, UMR 5023 LEHNA, F-69622

D J.B., 0009-0005-6000-7479; D.R., 0000-0002-8865-5428; Y.V., 0000-0003-0572-7199

et al., 2002; Porter and Brand, 1993, 1995; Porter et al., 1996; Roussel et al., 2015; Turner et al., 2005, 2006; Voituron et al.,

Mitochondria have a central role in global energy modulation, consuming approximately 90% of the oxygen inhaled by the organism to create a proton gradient across the inner mitochondrial membrane. Maintenance of this proton gradient involves the transfer of electrons through a series of complexes in which some electrons can leak to react with molecular oxygen and form incompletely reduced superoxide anion $(O_2^{\bullet-})$ and other downstream ROS. The proton gradient is used by the ATP synthase to generate ATP, a molecule that fuels nearly all of the physiological processes supporting the survival and performance of the organism. However, part of the proton gradient can also be dissipated by proton leak pathways, which divert energy away from ATP synthesis into heat production (Brand, 2000; Brand et al., 2005; Porter and Brand, 1993, 1995; Rolfe and Brown, 1997). The consequence of the proton leak is an alteration of the amount of ATP molecules synthesized by mitochondria for each oxygen atom consumed, i.e. the mitochondrial coupling efficiency (ATP/O ratio), and a reduction of the net ROS production. Therefore, mitochondrial coupling efficiency appears to be a key parameter of energy transduction, and variation in the efficiency of ATP production may have important consequences on individual performances (Koch et al., 2021; Salin et al., 2015).

In an allometric context, a study has shown that mitochondrial efficiency correlates positively with body mass in skeletal muscles of mammals, but this correlation depends on the metabolic intensity (Boel et al., 2019). Indeed, when the rate of ATP synthesis was reduced 40-fold, the mitochondrial efficiency dropped by 20-fold in the smallest mammals and by only 7-fold in the largest ones. Such a reduction of the coupling efficiency may favor heat generation, and thus help compensate for heat loss in small mammals, especially at rest. However, extending such 'activation' dependence to other tissues is still an open question. Here, we have hence focused on mitochondrial bioenergetics of skeletal and cardiac muscles, as both tissues are significant contributors to the standard metabolism of endotherms (Field et al., 1939; Konarzewski and Diamond, 1995; Raichlen et al., 2010) but exhibit different energetic requirements and metabolic scopes. Indeed, skeletal muscle is regularly subjected to different metabolic intensities because it can switch from a resting state to a maximal state to ensure locomotor function, whereas the heart muscle is always in an active state. Therefore, we investigated mitochondrial efficiency flexibility as a function of body mass in two muscle tissues that are contrasted in their range of activities. The aim of the present study was to explore mitochondrial bioenergetics (i.e. the triad of O₂ consumption, ATP synthesis and ROS generation) in addition to certain key enzyme activities of metabolic pathways (citrate synthase and lactate dehydrogenase) in the avian clade, through 13 bird species ranging from 15 g to 160 kg.

Villeurbanne, France *These authors contributed equally to this work

[‡]Author for correspondence (jessica.barbe@univ-lyon1.fr)

MATERIALS AND METHODS Animals and tissue sampling

All experiments were conducted in accordance with the animal care guidelines of the Ministère de la Recherche et de l'Enseignement Supérieur. We complied with Article R. 427-6 of the Environmental Code regarding wildlife species.

We selected 13 species of birds ranging from 15 g (zebra finch) to 160 kg (ostrich). Muscle tissues (skeletal muscle and heart) were acquired fresh and used for mitochondrial extraction. Ostriches (Struthio camelus), geese (Anser anser), ducks (Cairina moschata), pheasants (Phasianus colchicum), partridges (Perdix perdix) and quails (Coturnix japonica) were obtained from local breeders or slaughterhouses. Pigeons (Columba livia), rooks (Corvus frugilegus) and carrion crows (Corvus corone) were obtained from certified trappers (Associations des Piégeurs Agrées de l'Ain et du Rhône). Zebra finches (Taeniopygia guttata), budgerigars (Melopsittacus undulatus) and Bengali finches (Lonchura striata) were obtained from local providers and were killed by cervical dislocation. King penguins (Aptenodytes patagonicus) were captured during one austral summer campaign at the French Alfred Faure Station, Crozet archipelago (Possession Island, 46° 25'S, 51°45'E). According to the Agreed Measures for the Preservation of Antarctic and Sub-Antarctic Fauna and the ethical approval from the French Committee for Polar Research (IPEV program 131), superficial pectoralis muscle was surgically biopsied under general isoflurane anesthesia (heart was not sampled in this species). After surgery, the birds were allowed to recover in an outside enclosure for 4-7 days and then released at the site of their capture.

Mitochondrial isolation

Pectoralis and heart muscle samples (approximately 2 g) were collected, kept on ice-cold isolation buffer and used within 2 h for mitochondrial preparation. The ostrich is a flightless bird, and therefore we collected the gastrocnemius instead of the pectoralis, as was the case in all other flying and swimming species. Indeed, in the ostrich, the gastrocnemius is a primary locomotion muscle, i.e. running, and exhibits a relative proportional distribution muscle fibers type with a slight predominance of fast glycolytic fibers (Kohn et al., 2023; Velotto and Crasto, 2004). Skeletal muscle and heart mitochondrial populations were isolated in icecold isolation buffer (100 mmol l⁻¹ sucrose, 50 mmol l⁻¹ KCl, 5 mmol l⁻¹ EDTA and 50 mmol l⁻¹ Tris-base, pH 7.4), following a standard extraction protocol, using a Potter-Elvehjem homogenizer, protease digestion and differential centrifugation, all steps at 4°C. Briefly, muscle tissues were finely cut up, homogenized with a Potter-Elvehjem homogenizer (five passages) and centrifuged at 1000 g for 10 min. The supernatant containing subsarcolemmal mitochondria was conserved in an ice bath and the pellet containing intermyofibrillar mitochondria was suspended in isolation buffer and treated with protease from Bacillus licheniformis (1 mg g⁻¹ muscle wet mass) for 5 min in an ice bath. The homogenate was diluted (1:2) using the supernatant from the first centrifugation, and the mixture was centrifuged at 1000 g for 10 min. The resulting supernatant was filtered and centrifuged at 8700 g for 10 min to pellet the mitochondria. The mitochondrial pellet was then resuspended in isolation buffer and centrifuged at 8700 g for 10 min, and this wash step was repeated once. Protein concentrations were determined in the mitochondrial suspension using the BCA protein assay (Pierce, Thermo Fisher Scientific, France) with bovine serum albumin as the standard.

Mitochondrial oxidative phosphorylation efficiency

The mitochondrial oxidative phosphorylation efficiency was assessed at 40°C by measuring the rates of oxygen consumption (Clark oxygen electrode, Rank Brothers Ltd, UK) and ATP synthesis from the same mitochondrial aliquots. For Aptenodytes patagonicus, mitochondrial parameters were assayed at 38°C, and the values were recalculated to 40°C using a Q_{10} of 3.5 for oxygen consumption and 2.9 for the ATP synthesis rate (D. Roussel, personal data). Mitochondria were incubated in respiratory buffer (120 mmol l⁻¹ KCl, 5 mmol l⁻¹ KH₂PO₄, 2 mmol l⁻¹ MgCl₂, 1 mmol l⁻¹ EGTA, 3 mmol l⁻¹ HEPES and 0.3% BSA, pH 7.4) supplemented with an ADP-regenerating system consisting of 20 mmol l⁻¹ glucose and 2 U ml⁻¹ hexokinase. Respiration was initiated by adding a mixture of respiratory substrates comprising 5 mmol l^{-1} pyruvate, 2.5 mmol l^{-1} malate and 5 mmol l^{-1} succinate. After initial oxygen consumption was monitored, the active state of respiration was initiated by the addition of different amounts of ADP (5, 10, 20, 100 and 500 μ mol l⁻¹) describing different steady-state rates of phosphorylation. Alongside, the basal non-phosphorylating respiration rate was obtained by the addition of 2 ug ml⁻¹ oligomycin, an inhibitor of ATP synthase. Then, aliquots of mitochondrial suspension were withdrawn every minute and quenched in a perchloric acid solution (10% HClO₄, 25 mmol l⁻¹ EDTA). The denatured proteins were centrifuged at 21,000 g for 5 min at 4°C and the resulting supernatant was neutralized with a KOH solution (2 mol l⁻¹ KOH, 0.3 mol l⁻¹ Mops) and centrifuged at 21,000 g for 5 min (4°C). The ATP production was determined from the glucose-6-phosphate content of samples, as described previously (Teulier et al., 2010). Briefly, the supernatant was incubated in reaction buffer (50 mmol l⁻¹ triethanolamine-HCl, 7.5 mmol l⁻¹ MgCl₂ and 3.75 mmol l⁻¹ EDTA, pH 7.4, at room temperature) supplemented with 0.5 mmol l⁻¹ NAD and assayed spectrophotometrically by monitoring the production of NADH in the presence of 0.5 U glucose-6-phosphate dehydrogenase from Leuconostoc mesenteroides at 340 nm. The rate of ATP production was calculated from the slope of the linear accumulation of glucose-6-phosphate over the sampling time interval (1 min). It is important to note that the ATP synthesis was also determined in the basal non-phosphorylating respiration rates in the presence of 2 μg ml⁻¹ oligomycin to ensure that the measured rates were specific to the mitochondrial ATP synthase activity. These values were taken into account to calculate the rate of mitochondrial ATP synthesis. The mitochondrial coupling efficiency of oxidative phosphorylation, i.e. the ATP/O ratio, was determined by dividing the ATP synthesis rate by the oxygen consumption rate during state 3 respiration. The respiratory control ratio (RCR) was determined by dividing the maximum phosphorylating respiration measured in the presence of 500 $\mu mol \ l^{-1}$ ADP by the basal nonphosphorylating respiration measured in the presence of 2 μg ml⁻¹ oligomycin.

Mitochondrial reactive oxygen species generation

The rate of $\rm H_2O_2$ released by skeletal muscle and heart mitochondria was measured in respiratory buffer supplemented with 5 U ml $^{-1}$ horseradish peroxidase and 1 µmol l $^{-1}$ Amplex $^{\rm @}$ Red fluorescent dye at 40°C using a fluorometer at excitation and emission wavelengths of 560 and 584 nm, respectively. The rates of $\rm H_2O_2$ generation were recorded in the presence of substrates alone (5 mmol l $^{-1}$ pyruvate/2.5 mmol l $^{-1}$ malate/5 mmol l $^{-1}$ succinate, basal state) and after the addition of 500 µmol l $^{-1}$ ADP (active state). The fluorescent signal was finally calibrated using a standard curve obtained after successive addition of $\rm H_2O_2$.

Enzyme activities

Sub-samples (20-40 mg) of frozen skeletal muscle and heart were thawed and homogenized in ice-cold 100 mmol l⁻¹ phosphate buffer, pH 7.4. Homogenization was carried out using a 2010 Geno/ Grinder® tissue homogenizer (3×30 s, 20 s rest). Homogenized samples were diluted 1/11 in 100 mmol l⁻¹ phosphate buffer containing 0.02% BSA and then centrifuged at 1000 g for 10 min at 4°C. The supernatant containing citrate synthase (CS) and lactate dehydrogenase (LDH) was collected, and enzyme activities were assayed spectrophotometrically at 40°C. LDH activity was measured at 340 nm in a medium containing 20 mmol 1⁻¹ imidazole, 0.02% BSA and 280 µmol 1⁻¹ NADH (pH 7.4), and the reaction was initiated with 5 mmol l⁻¹ pyruvate. CS activity was measured at 412 nm in medium containing 100 mmol l⁻¹ TRIS buffer, 300 μ mol l⁻¹ acetyl-CoA and 100 μ mol l⁻¹ DTNB (pH 8), and the reaction was initiated by the addition of oxaloacetate $(400 \, \mu \text{mol} \, 1^{-1})$. The mitochondrial content of muscle tissues (milligrams of mitochondrial protein per milligram of tissue) was estimated by the ratio of CS activity measured in muscle tissue to that measured in isolated mitochondria. The LDH/CS ratio was calculated as an index of glycolytic capacity.

Statistical analyses

The phylogenetic tree of the bird species included in the study, as well as the method of acquisition, are presented in Fig. S1 and the Supplementary Materials and Methods. All analyses were performed in R version 4.2.1 (https://www.r-project.org/). We fitted our models using Bayesian phylogenetic mixed models from the MCMCglmm package (Hadfield, 2010). MCMCglmm uses a Markov chain Monte Carlo (MCMC) estimation approach and accounts for non-independence among closely related species by including the phylogenetic relationships among species as a random variable. We determined the number of iterations, thinning and burn-in period for each model run across the Hackett sequenced species phylogenetic tree (Hackett et al., 2008). Standard MCMCglmm diagnostic checks were performed for all models. We used a weakly informative prior with a set of parameters: v=0.002 and V=1. Variations in these parameters did not affect the results. We included the random effect of species, individual, season and bird status (domesticated or wild) and calculated the deviance information criteria (DIC) for each model. The model with only 'species' as a random effect had a much lower DIC value; therefore, the inclusion of the other random effects was not statistically justifiable. All the data were log₁₀ transformed to represent allometric relationships between body mass and mitochondrial parameters. The data were also translated into standard normal distribution to compare skeletal muscle and heart slopes. The coefficient of correlation r^2 was calculated as described previously (Nakagawa et al., 2014). We estimated the phylogenetic signal for each model and individual mitochondrial bioenergetics (Supplementary Materials and Methods) as an application condition for phylogenetic regressions. Posterior mean estimates (slopes; b) are presented with their 95% lower and upper credible intervals (CIs). P_{MCMC} with a very low values indicates strong significance of the coefficient away from zero, and $P_{\text{MCMC}} < 0.05$ was considered significant in this study.

RESULTS

Bioenergetic measurements were conducted on a total of 83 birds representing 13 species of 8 families and 7 orders (Struthioniformes, Sphenisciformes, Anseriformes, Galliformes, Columbiformes, Psittaciformes and Passeriformes). The body mass of the smallest

species (finch) differed by a factor of 10⁴ from the largest species (ostrich).

Mitochondrial oxygen consumption, ATP synthesis, and ROS production

Hypoallometric scaling (slope <1, negative allometry) between bird body mass and oxygen consumption, ATP synthesis and H₂O₂ production rates (see Table 1, Figs 1 and 2) was detected in both tissues. In skeletal muscle mitochondria, the rates of oxygen consumption [at both basal non-phosphorylating phosphorvlating (active) states] and the rate of ATP synthesis were negatively related to body mass, whereas the rates of mitochondrial H₂O₂ generation were not (Table 1, Fig. 1). In heart mitochondria, the allometric relationships were not significant, except for the generation of H₂O₂ in the basal and active states (Table 1, Fig. 2). Some species were not sampled for ROS production measurements in both tissues, particularly small species (finches) with regard to the cardiac muscle. This requires careful interpretation of the relationship between bird body mass and ROS production in both muscle tissues. The RCR values, calculated as the ratio between the maximal phosphorylating respiration and the basal non-phosphorylating respiration, were independent of bird body mass in both tissues (Table 1). On the whole, the mean±s.e.m. RCR value calculated for mitochondria isolated from skeletal muscles was 4.49±0.26, and that from the heart was 4.70 ± 0.39 .

Mitochondrial coupling efficiency

Mitochondrial efficiencies were measured at different steady states of phosphorylation and thus at different metabolic levels (Figs 1D and 2D). The data show positive allometry (slope >1) for the mitochondrial coupling efficiency only in skeletal muscle (Table 1) and at all metabolic intensities. For both the unstandardized and the standardized values, we found higher slopes corresponding to low metabolic intensities (slope_{eff400}=0.054; CIs=0.015 to 0.091; $slope_{eff200}=0.078$; CIs=0.023 to 0.125; $slope_{eff100}=0.093$; CIs=0.025 to 0.158; slope_{eff50}=0.099; CIs=0.035 to 0.179; and slope_{eff10}=0.135; CIs=0.029 to 0.229). Of note, the relationships between efficiency (ATP/O) and body mass for the highest intensities exhibited the strongest r^2 ($r_{\rm eff400}^2$ =0.57, $r_{\rm eff200}^2$ =0.56, $r_{\text{eff}100}^2 = 0.53$, $r_{\text{eff}50}^2 = 0.50$ and $r_{\text{eff}10}^2 = 0.49$), indicating that the data were well explained by the model and displayed less dispersion than for the lowest metabolic intensities. Interestingly, the dynamic transition from the basal to the maximal oxidative phosphorylation state occurred to a different extent in small versus large species. To evaluate this flexibility, we calculated the mitochondrial efficiency channelling factor (mtEC) by fitting the relationships between ATP/O ratios and the rates of ATP synthesis with a $mono\text{-exponential} \quad function \quad [ATP/O=P/O_{max}\times (1-e^{-mtEC\times JATP})],$ where J_{ATP} is the ATP synthesis rate and mtEC is the gradient of the non-linear curve (Boel et al., 2019). A strong and significant positive dependence of the mtEC factor on body mass was found in birds (Fig. 3), indicating that larger birds reach their maximum coupling efficiency faster than smaller birds. In heart mitochondria, the coupling efficiency was not dependent on metabolic levels and did not exhibit a significant relationship with body mass (Table 1, Fig. 2D). The mtEC factor values were also not related to body mass in heart mitochondria (Fig. 3).

Enzyme activities and mitochondrial content

On the whole, CS activities were negatively correlated with bird body mass in both muscle tissues, with a strong and significant

Table 1. Effect of body mass on mitochondrial parameters

	Skeletal muscle		Heart muscle	
	Posterior mean [95% CIs]	P_{MCMC}	Posterior mean [95% CIs]	P _{MCMC}
Oxygen consumption rate (nmol O ₂ min ⁻¹ mg ⁻¹ prof	tein)			
Active state	-0.573 [-1.02, -0.09]	0.02	-0.269 [-1.00, 0.45]	0.40
Basal state	-0.652 [-1.13, -0.18]	0.01	-0.163 [-1.01, 0.73]	0.69
ATP synthesis rate (nmol ATP min ⁻¹ mg ⁻¹ protein)				
Active state	-0.459 [-0.97, 0.01]	0.06	-0.233 [-1.06, 0.56]	0.53
H ₂ O ₂ generation rate (pmol H ₂ O ₂ min ⁻¹ mg ⁻¹ protei	n)			
Active state	-0.020 [-1.20, 1.37]	0.84	-0.409 [-2.16, 1.22]	0.65
Basal state	-0.459 [-0.97, 0.01]	0.10	-0.662 [-1.50, 0.08]	0.06
Ratios				
ATP/O _{eff400}	0.545 [0.21, 0.89]	<0.01	0.372 [-0.47, 1.17]	0.34
ATP/O _{eff200}	0.619 [0.21, 1.02]	<0.01	0.383 [-0.51, 1.20]	0.37
ATP/O _{eff100}	0.648 [0.26, 1.11]	<0.01	0.355 [-0.58, 1.34]	0.42
ATP/O _{eff50}	0.649 [0.21, 1.11]	< 0.01	0.309 [-0.50, 1.18]	0.47
ATP/O _{eff10}	0.649 [0.18, 1.09]	0.01	0.218 [-0.50, 1.28]	0.48
RCR	-0.003 [-0.04, 0.06]	0.89	-0.022 [-0.10, 0.06]	0.54

Mitochondrial ATP synthesis, oxygen consumption and H_2O_2 production rates were measured in skeletal muscle (n=68) and heart (n=47) mitochondria fuelled with pyruvate/malate/succinate (basal state) or ADP (active state). Mitochondrial coupling efficiency (ATP/ $O_{\rm eff}$) was measured at a given rate of ATP synthesis (400, 200, 100, 50 or 10 nmol ATP min⁻¹ mg⁻¹ protein). RCR values were calculated as the ratio between the maximal phosphorylating respiration and the basal non-phosphorylating respiration. The posterior mean represents the estimated slope (b) under the standard normal distribution of the allometric equation with lower and upper 95% credible intervals (CIs).

relationship in the heart (posterior mean=-0.101, CIs=-0.159 to -0.035, r^2 =0.56, P_{MCMC} =0.01), and a loose relationship in skeletal muscle (posterior mean=-0.204, CIs=-0.433 to 0.062, r^2 =0.24,

 $P_{\rm MCMC}$ =0.12). Similarly, mitochondrial CS activity appeared to scale negatively with body mass, showing a strong significant relationship in skeletal muscle (posterior mean=-0.078,

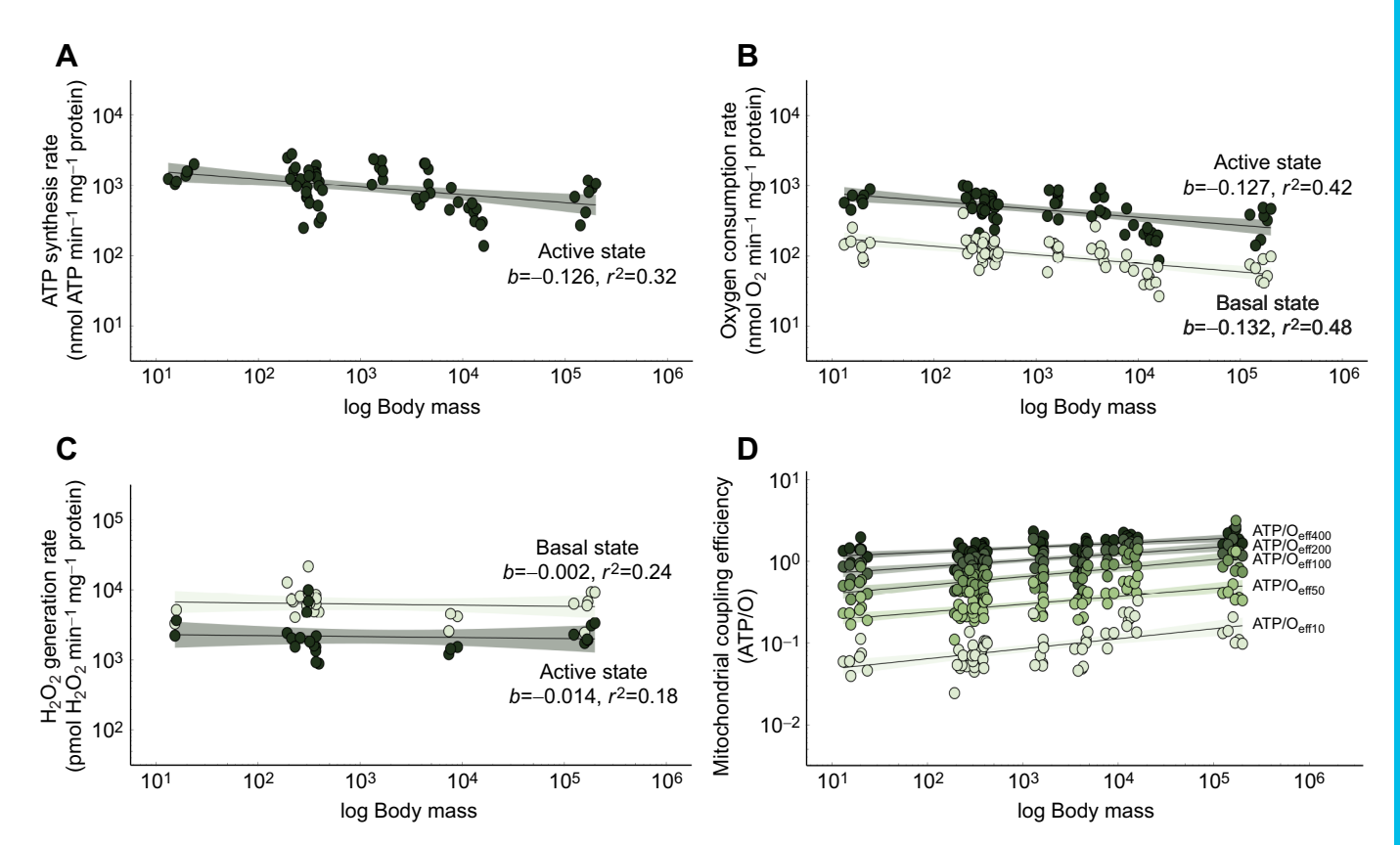


Fig. 1. Relationships between body mass (g) and mitochondrial fluxes and efficiency in the skeletal muscle. (A) Allometric relationships for ATP synthesis in mitochondria respiring on pyruvate/malate/succinate in the presence of 500 μ mol I⁻¹ ADP (active state). (B) Allometric relationships for oxygen consumption in mitochondria respiring on pyruvate/malate/succinate in the presence of oligomycin (basal non-phosphorylating state) or after the addition of 500 μ mol I⁻¹ ADP (active state). (C) Allometric relationships for H₂O₂ production rates in basal (respiratory substrates alone) or active states. (D) Relationships for mitochondrial effective coupling efficiencies (ATP/O_{eff}) calculated at a given rate of ATP synthesis (400, 200, 100, 50 or 10 nmol ATP min⁻¹ mg⁻¹ protein). Data were collected from 68 individuals from 11 bird species, except for the H₂O₂ production rate, for which only 27 individuals from 6 bird species were assayed.

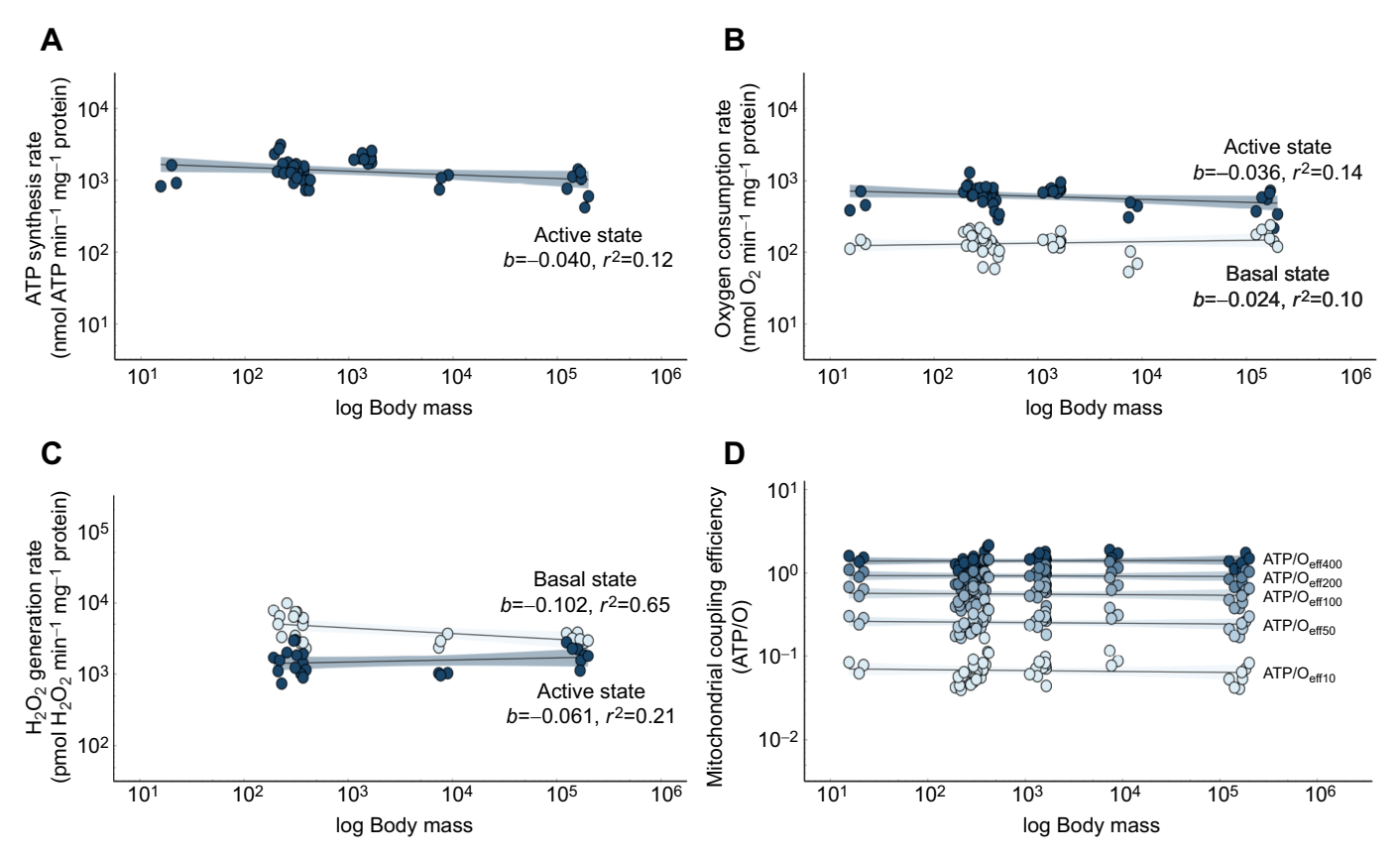


Fig. 2. Relationships between body mass (g) and mitochondrial fluxes and efficiency in the cardiac muscle. (A) Allometric relationships for ATP synthesis in mitochondria respiring on pyruvate/malate/succinate in the presence of 500 μ mol I⁻¹ ADP (active state). (B) Allometric relationships for oxygen consumption in mitochondria respiring on pyruvate/malate/succinate in the presence of oligomycin (basal non-phosphorylating state) or after the addition of 500 μ mol I⁻¹ ADP (active state). (C) Allometric relationships for H₂O₂ production rates in basal (respiratory substrates alone) or active states. (D) Relationships for mitochondrial effective coupling efficiencies (ATP/O_{eff}) calculated at a given rate of ATP synthesis (400, 200, 100, 50 or 10 nmol ATP min⁻¹ mg⁻¹ protein). Data were collected from 47 individuals from 9 bird species, except for the H₂O₂ production rate, for which only 24 individuals from 5 bird species were assayed.

CIs=-0.137 to -0.017, r^2 =0.65, $P_{\rm MCMC}$ =0.02) that was not found in the heart (posterior mean=-0.035, CIs=-0.106 to 0.034, r^2 =0.15, $P_{\rm MCMC}$ =0.28). LDH activities were positively related to body mass in both tissues (skeletal muscle: posterior mean=0.156, CIs=-0.006 to 0.318, r^2 =0.32, $P_{\rm MCMC}$ =0.059; heart: posterior mean=0.068; CIs=-0.09 to 0.22, r^2 =0.12, $P_{\rm MCMC}$ =0.39). The positive relationship between the LDH/CS ratio and body mass was significant in skeletal muscles but not in the heart (Fig. 4A). The mitochondrial content showed a negative correlation with body mass in both skeletal and heart muscles (Fig. 4B).

DISCUSSION

The aim of this study was to highlight interspecific allometric relationships between bird body mass and various mitochondrial bioenergetics, including efficiency in two of the body's most metabolically active tissues, namely the skeletal and cardiac muscles. The data show, for the first time, a tissue dependence of the body mass effect on mitochondrial ATP production and ATP/O, as significant allometric patterns were detected only in skeletal muscles. However, we also found a negative relationship between mitochondrial protein content and body mass in both skeletal muscles and the heart, meaning that smaller birds exhibit higher amount of mitochondria in their muscles than larger ones. This implies that the effect of body mass on mitochondrial fluxes (oxygen consumption and ATP synthesis) will be exacerbated at the level of the tissue, resulting in a stronger negative allometric

relationship in the skeletal muscle and, to a lesser extent, in the heart. In terms of sub-cellular $\rm O_2$ consumption, these results are congruent with previous studies that separately examined allometric relationships from different tissues of different species (Brand et al., 2003; Hochachka et al., 1988; Turner et al., 2005, 2006), thus providing evidence that the allometric relationships between body mass and sub-cellular bioenergetics are not uniformly present in every tissue and/or do not present with the same scaling exponent. In addition, in skeletal muscles, it appeared that the allometric pattern is dependent upon metabolic intensities, exhibiting a different degree of energetic flexibility between smaller and larger birds.

We collected pectoralis muscle tissue for each bird species (except for ostrich, for which we collected limb muscles) constituted of mixed glycolytic and oxidative muscle fibers, which resulted in samples with heterogeneously distributed fiber types. The pectoral muscle allows the wing to be folded down, but depending on the species, it is associated with different flight performances. Small birds, which have a high wing flapping frequency, have a pectoral muscle composed mainly of fast oxidative glycolytic fibers (Marquez et al., 2005; Welch and Altshuler, 2009), whereas larger, soaring or flightless birds have more heterogeneously distributed fiber types, with pectoral muscles also composed of slow oxidative and fast glycolytic fibers (Rosser and George, 1986; Rosser et al., 1993, 1996). In the present study, we reported that body mass is positively related to the ratios of LDH/CS and

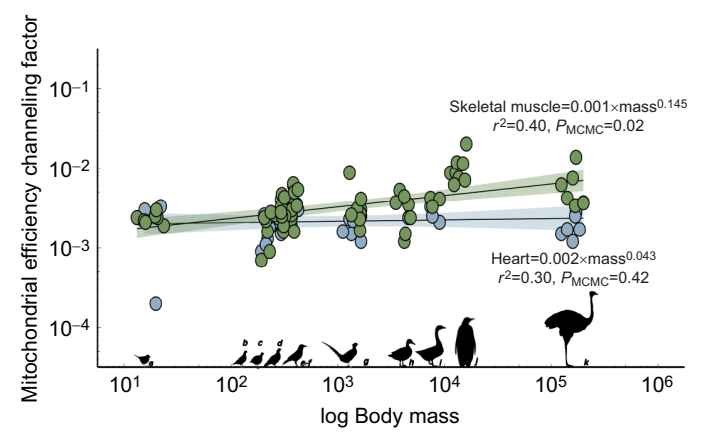


Fig. 3. Relationship between body mass (g) and mitochondrial efficiency channeling factor (mtEC) in skeletal and cardiac muscles. Allometric equations are represented for the heart (blue circles) and skeletal muscle (green circles). Data were calculated (see Results for more details) in 67 individuals from 11 bird species for skeletal muscles and in 47 individuals from 9 bird species for the heart. The silhouettes at the bottom illustrated the 11 species, which were: (1) Taeniopygia guttata, zebra finch; (2) Coturnix japonica, quail; (3) Columba livia, pigeon; (4) Perdix perdix, partridge; (5) Corvus frugilegus, rook; (6) Corvus corone, carrion crow; (7) Phasianus colchicum, pheasant; (8) Cairina moschata, duck; (9) Anser anser, goose; (10) Aptenodytes patagonicus, king penguin; and (11) Struthio camelus, ostrich.

negatively related to the mitochondrial content of the skeletal muscle, indicating a greater oxidative potential of skeletal muscles in smaller species than in larger birds. This scaling of oxidative/glycolytic enzyme activities or mitochondrial content has also been reported in mammals, indicating that the larger the endotherm the higher the glycolytic potential of its skeletal muscles (Else and Hulbert, 1985; Emmett and Hochachka, 1981). In turn, these data may suggest differences in fiber type composition of skeletal muscles between small and larger species. Even though small (less than 30%) fiber type differences for mitochondrial respiratory activity have been reported for complex I and/or complex II respiratory substrates (Bottje et al., 2002; Duchamp et al., 1991; Gueguen et al., 2005; Jackman and Willis, 1996; Mogensen and Sahlin, 2005; Picard et al., 2012), we cannot rule out that differences in fiber composition could explain part of the allometric scaling of

mitochondrial activities reported in the present study. This hypothesis is reinforced by the absence of an allometric pattern in the heart muscle. However, other mitochondrial parameters remain to be investigated, such as the surface area as well as the fatty acids and protein composition of the mitochondrial inner membrane, which may also contribute to the observed results (Brand et al., 2003, 2005; Hulbert et al., 2002, 2006).

In both skeletal muscles and heart tissue, mitochondria exhibited a higher coupling efficiency at high oxidative phosphorylation activity than at low mitochondrial activity (Figs 1D, 2D). This increase in mitochondrial coupling efficiency with the intensity of mitochondrial fluxes is well explained by the intrinsic kinetics of the proton leakage across the inner membrane. Mitochondria consume oxygen to build up a proton-motive force, which is then used by the ATP synthase to synthetize ATP. However, part of this protonmotive force, as well as the associated oxygen consumption, is not coupled to ATP synthesis and is instead consumed by nonproductive proton leak pathways (Rolfe and Brown, 1997). As a consequence, the activity of proton leakage negatively controls the mitochondrial coupling efficiency (Brand et al., 1993). Because the ATP synthase and proton leak pathways compete for the same driving force, the higher the phosphorylating activity is, the lower the proton leakage across the inner membrane would be, resulting in the highest coupling efficiency at maximal oxidative phosphorylation activity (Brand et al., 1993; Teulier et al., 2010; Boël et al., 2019). In situ, it has been reported that mitochondrial proton leakage contributes to a larger proportion of the oxygen consumed by perfused skeletal muscles in the resting state than in the working state, 50% versus 34%, respectively (Rolfe and Brand, 1996; Rolfe et al., 1999). The stronger decrease in coupling efficiency at low mitochondrial activity reported here in small birds may suggest a higher proton leakage than in larger birds. In turn, this suggests that mitochondrial proton conductance in skeletal muscles would depend negatively on body mass in birds. as previously shown for liver mitochondria (Brand et al., 2003). By comparison, proton leakage would contribute to a maximum of 13% of the oxygen consumed by the heart in vivo (Rolfe and Brown, 1997). This very low contribution of proton leak pathways to oxygen consumption in the heart could explain the absence of flexibility of the mitochondrial coupling efficiency in this organ. Nevertheless, further studies are needed to clarify this hypothesis.

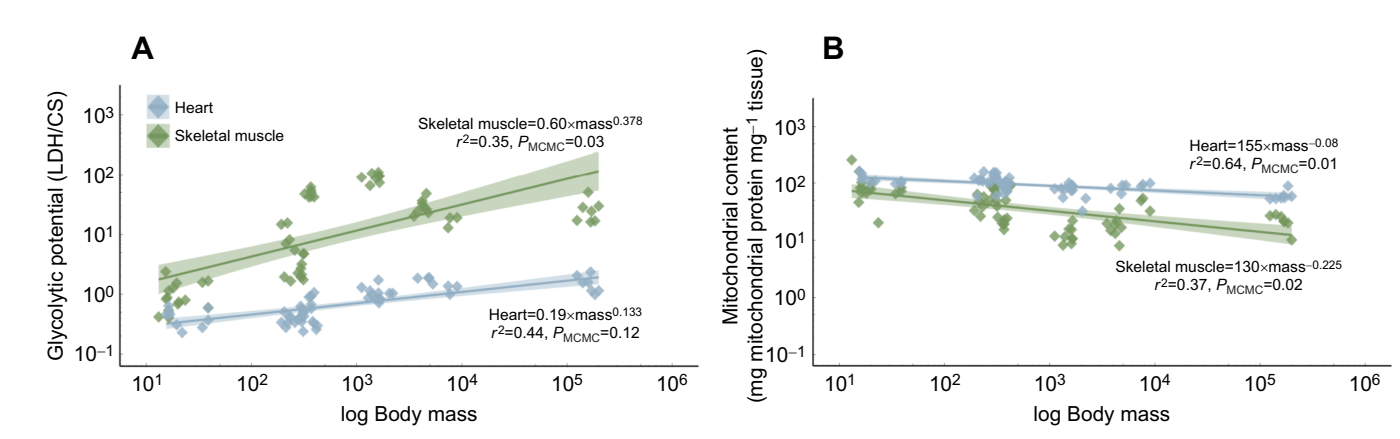


Fig. 4. Body mass dependence of glycolytic potential and mitochondrial content in the skeletal and cardiac muscles. (A) Allometric relationships for the glycolytic potential, calculated as the ratio between the activities of lactate dehydrogenase and citrate synthase (LDH/CS ratio). (B) Allometric relationships for the mitochondrial content (mg protein mg⁻¹ tissue). Data are from 73 individuals representing 12 bird species. Allometric equations are represented for the heart (blue diamonds) and skeletal muscle (green diamonds).

The difference in the scaling of mitochondrial parameters between skeletal muscle and heart may also result from differences in the metabolic scope and/or physiological function between the two tissues. An important feature of skeletal muscle is the massive potential to support a wide range of activities, from basal activity to rapidly increasing the rate of energy demand and consumption (Westerblad et al., 2010). Although the heart also undergoes modulations and responds to external stimuli (i.e. circadian rhythms, locomotion), it cannot be in a state of total rest, contrary to skeletal muscle, because of the necessity to generate regular vital contractions. Therefore, the heart often works at a relatively constant and high intensity to support its function regardless of body mass. Yet, allometric relationships have emerged in various avian studies (Bishop, 1997; Grubb, 1983) concerning morphological (i.e. heart mass) and physiological parameters (i.e. heartbeat frequency, output and stroke volume). The present study further highlights the effect of bird body mass on the oxidative capacity (CS activity) and mitochondrial content of the heart, which are higher in small birds than in larger avian species. Nevertheless, we did not find allometric patterns of mitochondrial fluxes (ATP synthesis, oxygen consumption and ROS production) and efficiency, suggesting that being a large bird has neither more nor less of an energetic advantage compared with being a small bird for the mitochondria of heart tissue. In endotherms, the skeletal muscle is an important site of thermogenesis (Block, 1994; Janský, 1973; Rowland et al., 2015). In this context, it is interesting to note the similar allometric patterns of mitochondrial coupling efficiency reported in the skeletal muscle of birds (present study) and mammals (Boël et al., 2019), showing that coupling efficiency in small birds and mammals falls at low metabolic intensities. This similarity can be viewed as a bioenergetics lever that would facilitate heat production in small endotherms at rest. Indeed, owing to their high surface-to-volume ratio, smaller endotherms have greater heat losses that necessitate compensatory increases in metabolic heat production to maintain the body temperature. This thermal constraint would be exacerbated at rest when activity is low. Therefore, it would be advantageous for smaller endotherms to further uncouple their skeletal muscle mitochondria in order to increase heat generation.

The 13 bird species included in this study exhibited a wide range of body masses, thrived in different environments, and in some cases had physiological differences that were challenging to account for. In this context, we should discuss some of the study's methodological and conceptual shortcomings. First, to standardize the measurement between all bird species, the isolated mitochondria of both tissues were tested at a temperature of 40°C. However, in the present study, the body temperature of large birds (ostriches and penguins) was generally lower than 40°C, whereas small birds (finches) tended to have body temperatures higher than 40°C (McNab, 1966). Flying birds also appear to have a higher body temperature than flightless birds (ostriches and penguins). By measuring mitochondrial parameters at a common temperature, we may have misestimated the optimal mitochondrial functioning in small (underestimation) and large birds (overestimation), which in turn would underestimate the allometric patterns. Such a potential temperature effect cannot affect our conclusions, and instead would reinforce the outcomes of the present study. Another methodological limitation may be the use of body mass as the sole morphological variable. Indeed, the wingspan could constitute another more informative morphological proxy, especially when investigating flight muscle bioenergetics. It would be useful to generate Bayesian models similar to those presented in this study

that consider the wingspan as another morphological variable. Even though the wingspan displays a positive allometry $(b^{1/3})$ relative to body mass (Nudds, 2007), it exhibits a lower phylogenetic signal (\sim 0.64) than the body mass does (see Supplementary Materials and Methods), decreasing the phylogenetic dependence of the morphological variable. Consequently, the wingspan would be an important and interesting parameter in bird allometric studies, which could provide complementary information to the variation of some mitochondrial energetic parameters.

In conclusion, the present work highlights the tissue-dependent effect of bird body mass on mitochondrial bioenergetics. Although the mitochondrial coupling efficiency in skeletal muscles correlated positively with bird body mass and depended on the metabolic intensity, the picture for cardiac muscles is simpler as there was no allometric pattern. As discussed above, the difference in the flexibility of the mitochondrial coupling efficiency between skeletal muscles and heart might be linked with the thermogenesis role of the skeletal muscle and the need for small endotherms to maintain heat generation at rest. Although this thermoregulatory hypothesis is attractive, the reason why coupling efficiency is more flexible in mitochondria from tissues with greater ranges of metabolic activity, such as skeletal muscles (present study; Boël et al., 2019), and less flexible in tissue with lower ranges of metabolic activity, such as the heart (present study) or liver (Boël et al., 2023), remains unknown. In perspective, it is interesting to note that cultured cells often show no allometry, suggesting that some systemic effect has been lost (Glazier, 2015a,b). Thus, the tissue-dependent effect of bird body mass on mitochondrial bioenergetics suggests that scaling cellular properties with body mass would also be influenced by some systemic effects, which remains to be clarified. Such a hypothesis is in agreement with recent literature arguing that metabolism scaling explanations must extend beyond simple energetic or physical constraints and take into account other parameters such as lifehistory traits (White et al., 2022; Giancarli et al., 2023).

Acknowledgements

We thank certified trappers from the UNAPAF association (Union National des Associations de Piégeurs Agréés) for providing pigeons and corvids and local providers and farmers for providing all the other birds in this study. We warmly thank the two reviewers for their constructive remarks and comments on the manuscript.

Competing interests

The authors declare no competing or financial interests.

Author contributions

Conceptualization: D.R., Y.V.; Methodology: J.B., D.R., Y.V.; Validation: J.B., D.R., Y.V.; Formal analysis: J.B.; Investigation: J.B., J.W., D.R., Y.V.; Writing - original draft: J.B.; Writing - review & editing: J.B., D.R., Y.V.; Visualization: J.B., D.R., Y.V.

Funding

J.B. was supported by the French Government (PhD grant: 2020–2023).

Data availability

Code and data are available from Zenodo: https://doi.org/10.5281/zenodo.8355492.

References

Bishop, C. M. (1997). Heart mass and the maximum cardiac output of birds and mammals: implications for estimating the maximum aerobic power input of flying animals. *Philos. Trans. R. Soc. Lond. B Biol. Sci.* 352, 447-456. doi:10.1098/rstb. 1997.0032

Block, B. A. (1994). Thermogenesis in muscle. Annu. Rev. Physiol. 56, 535-577. doi:10.1146/annurev.ph.56.030194.002535

Boël, M., Romestaing, C., Voituron, Y. and Roussel, D. (2019). Allometry of mitochondrial efficiency is set by metabolic intensity. *Proc. R. Soc. B Biol. Sci.* 286, 20191693. doi:10.1098/rspb.2019.1693

Boël, M., Voituron, Y. and Roussel, D. (2023). Body mass dependence of oxidative phosphorylation efficiency in liver mitochondria from mammals. *Comp. Biochem. Physiol.* 284A, 111490. doi:10.1016/j.cbpa.2023.111490

- Bottje, W., Iqbal, M., Tang, Z. X., Cawthon, D., Okimoto, R., Wing, T. and Cooper, M. (2002). Association of mitochondrial function with feed efficiency within a single genetic line of male broilers. *Poult. Sci.* 81, 546-555. doi:10.1093/ps/81.4.546
- Brand, M. D. (2000). Uncoupling to survive? The role of mitochondrial inefficiency in ageing. Exp. Gerontol. 35, 811-820. doi:10.1016/S0531-5565(00)00135-2
- Brand, M. D., Harper, M. E. and Taylor, H. C. (1993). Control of the effective P/O ratio of oxidative phosphorylation in liver mitochondria and hepatocytes. *Biochem. J.* 291, 739-748. doi:10.1042/bj2910739
- Brand, M. D., Turner, N., Ocloo, A., Else, P. L. and Hulbert, A. J. (2003). Proton conductance and fatty acyl composition of liver mitochondria correlates with body mass in birds. *Biochem. J.* 376, 741-748. doi:10.1042/bj20030984
- Brand, M. D., Pakay, J. L., Ocloo, A., Kokoszka, J., Wallace, D. C., Brookes, P. S. and Cornwall, E. J. (2005). The basal proton conductance of mitochondria depends on adenine nucleotide translocase content. *Biochem. J.* 392, 353-362. doi:10.1042/BJ20050890
- Calder, W. A. (1996). Size, Function, and Life History. Mineola, NY: Dover Publications.
- Darveau, C.-A., Suarez, R. K., Andrews, R. D. and Hochachka, P. W. (2002).
 Allometric cascade as a unifying principle of body mass effects on metabolism.
 Nature 417, 166-170. doi:10.1038/417166a
- **Demetrius, L.** (2006). The origin of allometric scaling laws in biology. *J. Theor. Biol.* **243**, 455-467. doi:10.1016/j.jtbi.2006.05.031
- Duchamp, C., Barre, H., Rouanet, J. L., Lanni, A., Cohen-Adad, F., Berne, G. and Brebion, P. (1991). Nonshivering thermogenesis in king penguin chicks. I. Role of skeletal muscle. *Am. J. Physiol. Regul. Integr. Comp. Physiol.* 261, R1438-R1445. doi:10.1152/ajpregu.1991.261.6.R1438
- Else, P. L. and Hulbert, A. J. (1985). An allometric comparison of the mitochondria of mammalian and reptilian tissues: the implications for the evolution of endothermy. J. Comp. Physiol. B 156, 3-11. doi:10.1007/BF00692920
- Else, P. L., Brand, M. D., Turner, N. and Hulbert, A. J. (2004). Respiration rate of hepatocytes varies with body mass in birds. *J. Exp. Biol.* **207**, 2305-2311. doi:10. 1242/jeb.01017
- Emmett, B. and Hochachka, P. W. (1981). Scaling of oxidative and glycolytic enzymes in mammals. *Respir. Physiol.* 45, 261-272. doi:10.1016/0034-5687(81)90010-4
- Field, J., , 2nd, Belding, H. S. and Martin, A. W. (1939). An analysis of the relation between basal metabolism and summated tissue respiration in the rat. I. The post-pubertal albino rat. J. Cell. Comp. Physiol. 14, 143-157. doi:10. 1002/jcp.1030140202
- Giancarli, S. M., Dunham, A. E. and O'connor, M. P. (2023). Clade-specific allometries in avian basal metabolic rate demand a broader theory of allometry. *Physiol. Biochem. Zool.* **96**, 216-232. doi:10.1086/725207
- Glazier, D. S. (2015a). Is metabolic rate a universal 'pacemaker' for biological processes? *Biol. Rev.* **90**, 377-407. doi:10.1111/brv.12115
- Glazier, D. (2015b). Body-mass scaling of metabolic rate: what are the relative roles of cellular versus systemic effects? *Biology* 4, 187-199. doi:10.3390/ biology4010187
- Glazier, D. S. (2022). Variable metabolic scaling breaks the law: from 'Newtonian' to 'Darwinian' approaches. *Proc. R. Soc. B.* **289**, 20221605. doi:10.1098/rspb.2022. 1605
- Grubb, B. R. (1983). Allometric relations of cardiovascular function in birds. Am. J. Physiol. Heart Circ. Physiol. 245, H567-H572. doi:10.1152/ajpheart.1983. 245.4.H567
- Gueguen, N., Lefaucheur, L., Fillaut, M. and Herpin, P. (2005). Muscle fiber contractile type influences the regulation of mitochondrial function. *Mol. Cell. Biochem.* 276, 15-20. doi:10.1007/s11010-005-2464-y
- Hackett, S. J., Kimball, R. T., Reddy, S., Bowie, R. C. K., Braun, E. L., Braun, M. J., Chojnowski, J. L., Cox, W. A., Han, K.-L., Harshman, J. et al. (2008). A phylogenomic study of birds reveals their evolutionary history. *Science* 320, 1763-1768. doi:10.1126/science.1157704
- Hadfield, J. D. (2010). MCMC methods for multi-response generalized linear mixed models: the MCMCglmm R package. J. Stat. Softw. 33, 1-22. doi:10.18637/jss. v033.i02
- Hatton, I. A., Dobson, A. P., Storch, D., Galbraith, E. D. and Loreau, M. (2019). Linking scaling laws across eukaryotes. *Proc. Natl. Acad. Sci. USA* 116, 21616-21622. doi:10.1073/pnas.1900492116
- Hochachka, P. W., Emmett, B. and Suarez, R. K. (1988). Limits and constraints in the scaling of oxidative and glycolytic enzymes in homeotherms. *Can. J. Zool.* 66, 1128-1138. doi:10.1139/z88-165
- Hulbert, A. J., Faulks, S., Buttemer, W. A. and Else, P. L. (2002). Acyl composition of muscle membranes varies with body size in birds. J. Exp. Biol. 205, 3561-3569. doi:10.1242/jeb.205.22.3561
- Hulbert, A. J., Turner, N., Hinde, J., Else, P. and Guderley, H. (2006). How might you compare mitochondria from different tissues and different species? *J. Comp. Physiol. B* 176, 93-105. doi:10.1007/s00360-005-0025-z
- Hulbert, A. J., Pamplona, R., Buffenstein, R. and Buttemer, W. A. (2007). Life and death: metabolic rate, membrane composition, and life span of animals. *Physiol. Rev.* 87, 1175-1213. doi:10.1152/physrev.00047.2006

- Jackman, M. R. and Willis, W. T. (1996). Characteristics of mitochondria isolated from type I and type IIb skeletal muscle. Am. J. Physiol. Cell Physiol. 270, C673-C678. doi:10.1152/ajpcell.1996.270.2.C673
- Janský, L. (1973). Non-shivering thermogenesis and its thermoregulatory significance. Biol. Rev. 48, 85-132. doi:10.1111/j.1469-185X.1973.tb01115.x
- Koch, R. E., Buchanan, K. L., Casagrande, S., Crino, O., Dowling, D. K., Hill, G. E., Hood, W. R., Mckenzie, M., Mariette, M. M., Noble, D. W. A. et al. (2021). Integrating mitochondrial aerobic metabolism into ecology and evolution. *Trends Ecol. Evol.* 36, 321-332. doi:10.1016/j.tree.2020.12.006
- Kohn, T. A., Anley, M. J., Magwaza, S. N., Adamson, L., Hoffman, L. C. and Brand, T. S. (2023). Muscle fiber type and metabolic profiles of four muscles from the African black ostrich. *Meat Sci.* 200, 109156. doi:10.1016/j.meatsci.2023. 109156
- Konarzewski, M. and Diamond, J. (1995). Evolution of basal metabolic rate and organ masses in laboratory mice. *Evolution* **49**, 1239-1248. doi:10.2307/2410448
- Marquez, J., Sweazea, K. L. and Braun, E. J. (2005). Skeletal muscle fiber composition of the English sparrow (Passer domesticus). Comp. Biochem. Physiol. B Biochem. Mol. Biol. 143, 126-131. doi:10.1016/j.cbpb.2005.10.011
- McNab, B. K. (1966). An analysis of the body temperatures of birds. Condor 68, 47-55. doi:10.2307/1365174
- Mogensen, M. and Sahlin, K. (2005). Mitochondrial efficiency in rat skeletal muscle: influence of respiration rate, substrate and muscle type. *Acta Physiol. Scand.* **185**, 229-236. doi:10.1111/j.1365-201X.2005.01488.x
- Nakagawa, S., Johnson, P. C. D. and Schielzeth, H. (2014). The coefficient of determination R2 and intra-class correlation coefficient from generalized linear mixed-effects models revisited and expanded. J. R. Soc. Interface 11, 20170213. doi:10.1098/rsif.2017.0213
- Nudds, R. L. (2007). Wing-bone length allometry in birds. J. Avian Biol. 38, 515-519. doi:10.1111/j.0908-8857.2007.03913.x
- Peters, R. H. (1983). The Ecological Implications of Body Size. Cambridge University Press.
- Picard, M., Hepple, R. T. and Burelle, Y. (2012). Mitochondrial functional specialization in glycolytic and oxidative muscle fibers: tailoring the organelle for optimal function. *Am. J. Physiol. Cell Physiol.* **302**, C629-C641. doi:10.1152/ajpcell.00368.2011
- Porter, R. K. and Brand, M. D. (1993). Body mass dependence of H⁺ leak in mitochondria and its relevance to metabolic rate. *Nature* 362, 628-630. doi:10. 1038/362628a0
- Porter, R. K. and Brand, M. D. (1995). Causes of differences in respiration rate of hepatocytes from mammals of different body mass. *Am. J. Physiol. Regul. Integr. Comp. Physiol.* 269, R1213-R1224. doi:10.1152/ajpregu.1995.269.5.R1213
- Porter, R. K., Hulbert, A. J. and Brand, M. D. (1996). Allometry of mitochondrial proton leak: influence of membrane surface area and fatty acid composition. Am. J. Physiol. Regul. Integr. Comp. Physiol. 271, R1550-R1560. doi:10.1152/ajpregu.1996.271.6.R1550
- Raichlen, D. A., Gordon, A. D., Muchlinski, M. N. and Snodgrass, J. J. (2010). Causes and significance of variation in mammalian basal metabolism. *J. Comp. Physiol. B* 180, 301-311. doi:10.1007/s00360-009-0399-4
- Rolfe, D. F. and Brand, M. D. (1996). Contribution of mitochondrial proton leak to skeletal muscle respiration and to standard metabolic rate. Am. J. Physiol. Cell Physiol. 271, C1380-C1389. doi:10.1152/ajpcell.1996.271.4.C1380
- Rolfe, D. F. and Brown, G. C. (1997). Cellular energy utilization and molecular origin of standard metabolic rate in mammals. *Physiol. Rev.* 77, 731-758. doi:10.1152/ physrev.1997.77.3.731
- Rolfe, D. F. S., Newman, J. M. B., Buckingham, J. A., Clark, M. G. and Brand, M. D. (1999). Contribution of mitochondrial proton leak to respiration rate in working skeletal muscle and liver and to SMR. Am. J. Physiol. Cell Physiol. 276, C692-C699. doi:10.1152/aipcell.1999.276.3.C692
- Rosser, B. W. C. and George, J. C. (1986). The avian pectoralis: histochemical characterization and distribution of muscle fiber types. *Can. J. Zool.* 64, 1174-1185. doi:10.1139/z86-176
- Rosser, B. W. C., Waldbillig, D. M., Wick, M. and Bandman, E. (1993). Muscle fiber types in the pectoralis of the white pelican, a soaring bird. *Acta Zool.* **75**, 329-336. doi:10.1111/j.1463-6395.1994.tb00970.x
- Rosser, B. W. C., Waldbillig, D. M., Wick, M. and Bandman, E. (1996). Heterogeneity of myosin heavy-chain expression in fast-twitch fiber types of mature avian pectoralis muscle. *Biochem. Cell Biol.* 74, 715-728. doi:10.1139/o96-078
- Roussel, D., Salin, K., Dumet, A., Romestaing, C., Rey, B. and Voituron, Y. (2015). Oxidative phosphorylation efficiency, proton conductance and reactive oxygen species production of liver mitochondria correlates with body mass in frogs. J. Exp. Biol. 218, 3222-3228. doi:10.1242/jeb.126086
- Rowland, L. A., Bal, N. C. and Periasamy, M. (2015). The role of skeletal-muscle-based thermogenic mechanisms in vertebrate endothermy. *Biol. Rev.* 90, 1279-1297. doi:10.1111/brv.12157
- Salin, K., Auer, S. K., Rey, B., Selman, C. and Metcalfe, N. B. (2015). Variation in the link between oxygen consumption and ATP production, and its relevance for animal performance. *Proc. R. Soc. B Biol. Sci.* 282, 20151028. doi:10.1098/rspb. 2015.1028

- Teulier, L., Rouanet, J.-L., Letexier, D., Romestaing, C., Belouze, M., Rey, B., Duchamp, C. and Roussel, D. (2010). Cold-acclimation-induced non-shivering thermogenesis in birds is associated with upregulation of avian UCP but not with innate uncoupling or altered ATP efficiency. *J. Exp. Biol.* 213, 2476-2482. doi:10. 1242/jeb.043489
- Turner, N., Haga, K. L., Hulbert, A. J. and Else, P. L. (2005). Relationship between body size, Na⁺/K⁺/ATPase activity, and membrane lipid composition in mammal and bird kidney. *Am. J. Physiol. Regul. Integr. Comp. Physiol.* **288**, R301-R310. doi:10.1152/ajpregu.00297.2004
- Turner, N., Haga, K. L., Else, P. L. and Hulbert, A. J. (2006). Scaling of Na⁺,K⁺-ATPase molecular activity and membrane fatty acid composition in mammalian and avian hearts. *Physiol. Biochem. Zool.* **79**, 522-533. doi:10.1086/502815
- Velotto, S. and Crasto, A. (2004). Histochemical and morphometrical characterization and distribution of fibre types in four muscles of ostrich (Struthio camelus). Anat. Histol. Embryol. 33, 251-256. doi:10.1111/j.1439-0264.2004.00535.x
- Voituron, Y., Boël, M. and Roussel, D. (2020). Mitochondrial threshold for H₂O₂ release in skeletal muscle of mammals. *Mitochondrion* 54, 85-91. doi:10.1016/j.mito.2020.07.005

- Welch, K. C. and Altshuler, D. L. (2009). Fiber type homogeneity of the flight musculature in small birds. Comp. Biochem. Physiol. B Biochem. Mol. Biol. 152, 324-331. doi:10.1016/j.cbpb.2008.12.013
- West, G. B. and Brown, J. H. (2004). Life's universal scaling laws. *Phys. Today* **57**, 36-42. doi:10.1063/1.1809090
- West, G. B. and Brown, J. H. (2005). The origin of allometric scaling laws in biology from genomes to ecosystems: towards a quantitative unifying theory of biological structure and organization. J. Exp. Biol. 208, 1575-1592. doi:10.1242/jeb.01589
- Westerblad, H., Bruton, J. D. and Katz, A. (2010). Skeletal muscle: energy metabolism, fiber types, fatigue and adaptability. Exp. Cell Res. 316, 3093-3099. doi:10.1016/j.yexcr.2010.05.019
- White, C. R., Marshall, D. J., Alton, L. A., Arnold, P. A., Beaman, J. E., Bywater, C. L., Condon, C., Crispin, T. S., Janetzki, A., Pirtle, E. et al. (2019). The origin and maintenance of metabolic allometry in animals. *Nat. Ecol. Evol.* 3, 598-603. doi:10.1038/s41559-019-0839-9
- White, C. R., Alton, L. A., Bywater, C. L., Lombardi, E. J. and Marshall, D. J. (2022). Metabolic scaling is the product of life-history optimization. *Science* **377**, 834-839. doi:10.1126/science.abm7649

Supplementary Materials and Methods

Phylogenetic tree

The phylogenetic tree (S1) combining the 13 species studied was obtained from the BirdTree.org website (Rubolini et al., 2015). The tree source used was Hackett Sequenced Species: a set of 10 000 trees with 6670 OTUs each (Hackett et al., 2008). We performed 1000 simulations to create the most parsimonious tree. The avian tree was summarized using BEAST platform (Bayesian Evolutionary Analysis Sampling Trees- v1.10.4, 2002-2018) to create a target tree usable in nexus format in R version 4.2.1 (R Core Team 2022). The parameters used were: burnin as a number of trees (100), maximum clade credibility tree as target tree type, and common ancestor heights.

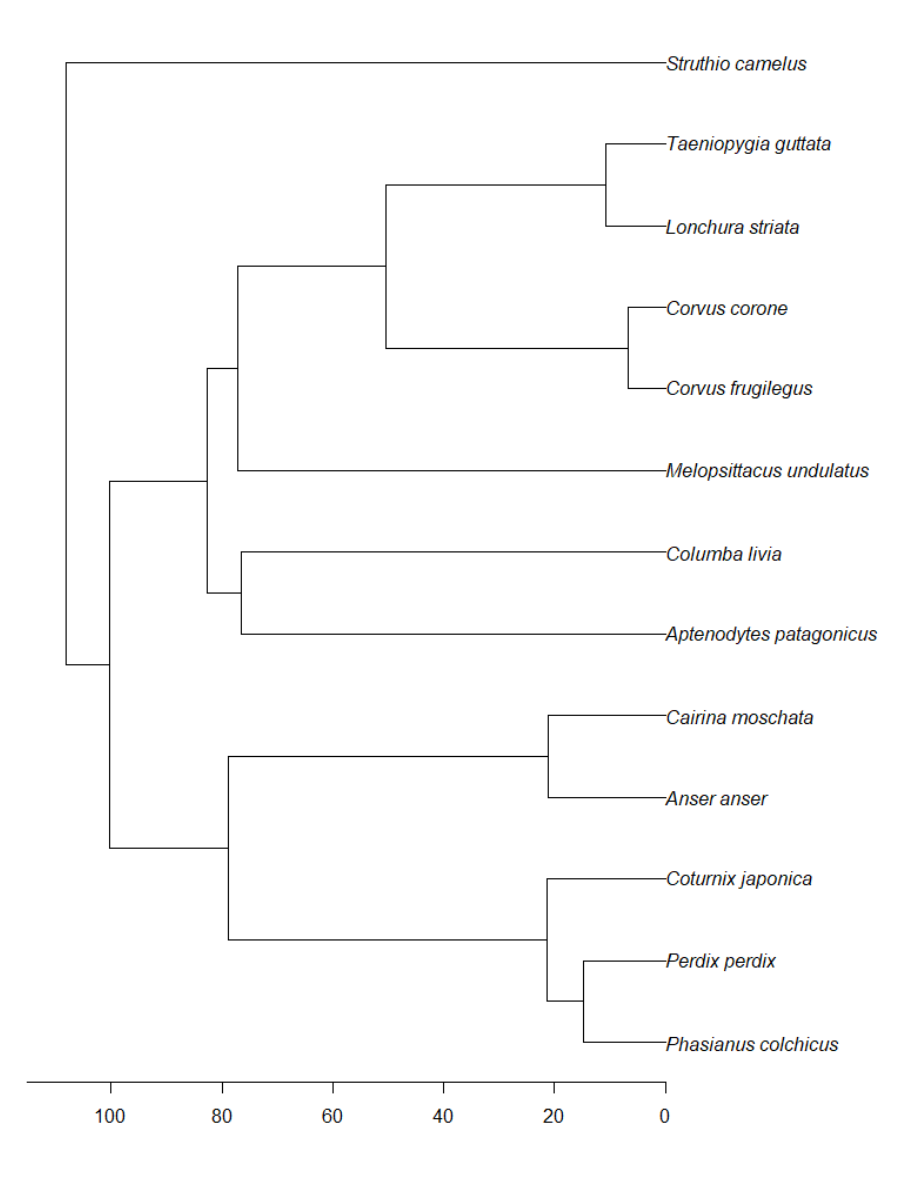


Fig. S1. Avian phylogeny of studied birds, with species names.

Phylogenetic signal of mitochondrial allometric models

The phylogenetic signal can be defined as the tendency for related species to resemble each other more than those drawn randomly from a phylogenetic tree (Blomberg et al., 2003). Moreover, the phylogenetic signal can be considered a measure of phylogenetic heritability (h^2) with a value that lies between 0 and 1. We obtained an estimate of the heritability by applying the basic formula from (de Villemereuil, 2019):

$$h^2 = \frac{V_{Additive \ variance}}{V_{Additive \ variance} \ + \ V_{Random \ effect \ variance} \ + \ V_{Residual \ variance}}$$

A value close to zero indicates phylogenetic independence and a value close to 1 indicates species' traits are distributed as expected under the Brownian motion model. Although h^2 was estimated using high likelihood (95% to lies between lower and upper credible interval) we did not test whether h^2 was significantly different from zero (i.e., there was no phylogenetic signal) but were able to estimate the strength of the correlation between certain mitochondrial traits and bird body mass and how the phylogeny affected the error structure of the data. Body mass exhibited a strong phylogenetic signal (h^2 = 0.997; CIs=0.995 to 0.999). In the allometric models, the phylogenetic signal of the different mitochondrial parameters relative to body mass or wingspan was generally > 0, indicating a non-negligible phylogenetic signal. The allometric relationships exhibited in this paper must be considered in conjunction with the phylogenetic signal specific to mitochondrial parameters. Heritability values estimated for each parameter are generally greater than 0.50 and represent a relatively strong phylogenetic signal (S2). It could then be that there is auto-collinearity between the different traits and that the significant relationships between the body mass and the mitochondrial parameter are partly due to the phylogenetic factor.

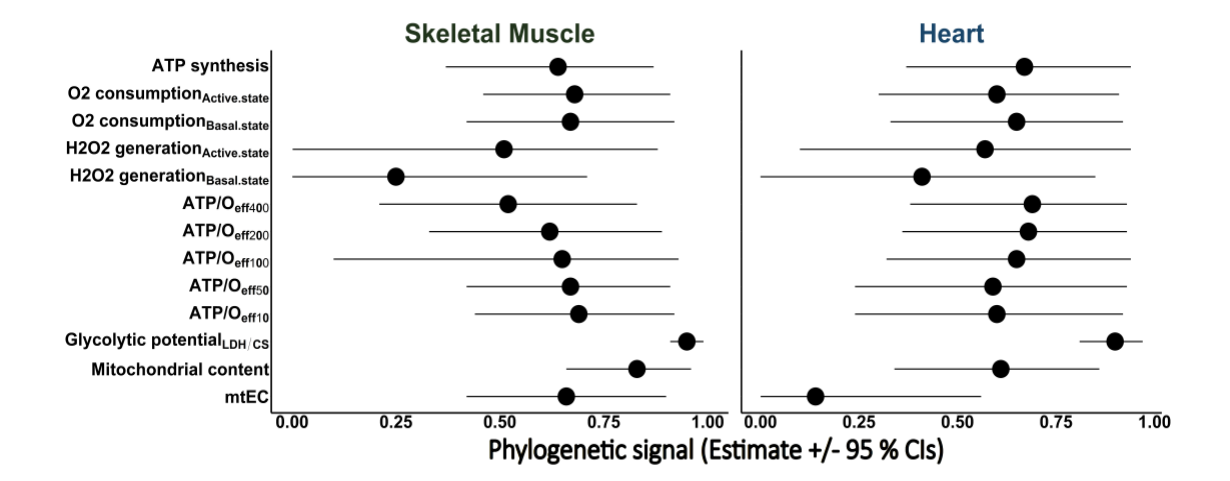


Fig. S2. Phylogenetic signal of mitochondrial allometric models for the avian skeletal and heart muscles, considering body mass as the variable.

References

Blomberg, S. P., Garland, T. and Ives, A. R. (2003). Testing for Phylogenetic Signal in Comparative Data: Behavioral Traits Are More Labile. *Evolution* **57**, 717–745.

de Villemereuil, P. (2019). On the relevance of Bayesian statistics and MCMC for animal models. *J. Anim. Breed. Genet.* **136**, 339–340.

Hackett, S. J., Kimball, R. T., Reddy, S., Bowie, R. C. K., Braun, E. L., Braun, M. J., Chojnowski, J. L., Cox, W. A., Han, K.-L., Harshman, J., et al. (2008). A Phylogenomic Study of Birds Reveals Their Evolutionary History. *Science* **320**, 1763–1768.

Rubolini, D., Liker, A., Garamszegi, L. Z., Møller, A. P. and Saino, N. (2015). Using the BirdTree.org website to obtain robust phylogenies for avian comparative studies: A primer. *Curr. Zool.* **61**, 959–965.